Chemical and Process Engineering Research
ISSN 2224-7467 (Paper) ISSN 2225-0913 (Online)
Vol.54, 2017

Simulation of a Naphtha Reforming Reactor

[1]Akpa, Jackson Gunorubon and Adeloye, Olalekan Michael[2]
Department of Chemical/Petrochemical Engineering,
Rivers State University, Port-Harcourt,
Rivers State, Nigeria
[1](corresponding author: akpa.jackson@ust.edu.ng), [2](adeloye.olalekan@yahoo.com)

ABSTRACT

Mathematical models for the reforming reactors of a Catalytic Reforming Unit were developed. The models were developed from first principles (conservation of mass and energy). The developed models were ordinary differential equations; were solved using ODE 45 solver of MATLAB and validated using plant data from the Catalytic Reforming reactor of the Port-Harcourt Refinery Company, Nigeria. The results gave a minimum percentage absolute error (deviation) between model predictions and industrial plant results of 0.0026% for inlet temperature, a maximum of 5.8% for Naphthene concentration; 2.1%, 2.2% and 1.6% for the concentrations of Aromatics, Paraffin and Hydrogen respectively. These shows that the model developed predicted the output of the catalytic reforming reactor very closely. The models were used to study the effect of process parameters such as inlet feed temperature, reactor pressure and the feed flow rate on the performance of the reforming reactor.

Keywords: Catalytic Naphtha Reforming, Modeling, Simulation.

1. Introduction

The Catalytic reforming unit transforms straight run low octane Naphtha from the crude distillation unit (CDU) into high-octane liquid products called reformates which are used as blending stocks with gasoline produced from other units of the refinery. This is accomplished through the conversion of linear alkane hydrocarbons (paraffins) into branched alkanes (iso-paraffins) and the partially dehydrogenation of cyclic naphthenes (cycloalkanes) to produce high-octane aromatic hydrocarbons occurring with a relatively small change in the boiling range as the hydrocarbon molecular structures are simply rearranged with minimal amount of cracking (Gary *et al*., 2007).

The Octane number is a fundamental characteristic of motor fuel and is the ability or resistance of a fuel to knocking in comparison to the antiknock quality of iso-octane, hence the higher the octane number of a gasoline the higher the compression ratio the fuel can withstand before detonating (PHRC, 1990). The enhancement of the octane number is achieved by the formation of aromatic compounds through several reactions, such as dehydrogenation, isomerization, cyclization and hydro-cracking; producing hydrogen (H_2) and liquefied petroleum gas (LPG) as by-products (Liang *et al*., 2005). The branched and aromatic hydrocarbons are less prone to ignite prematurely in internal combustion engines thus reduce knocking drastically.

The objective of this research is to develop through the application of the principle of conservation of mass and energy, mathematical models that will predict the conversion patterns and temperature progression of the reactors of a catalytic reforming unit.

1.1. Process Description

A simplified process scheme of the continuous reforming process used in the Port-Harcourt Refining Company, Rivers State, Nigeria (PHRC, 1990) is shown Figure 1.

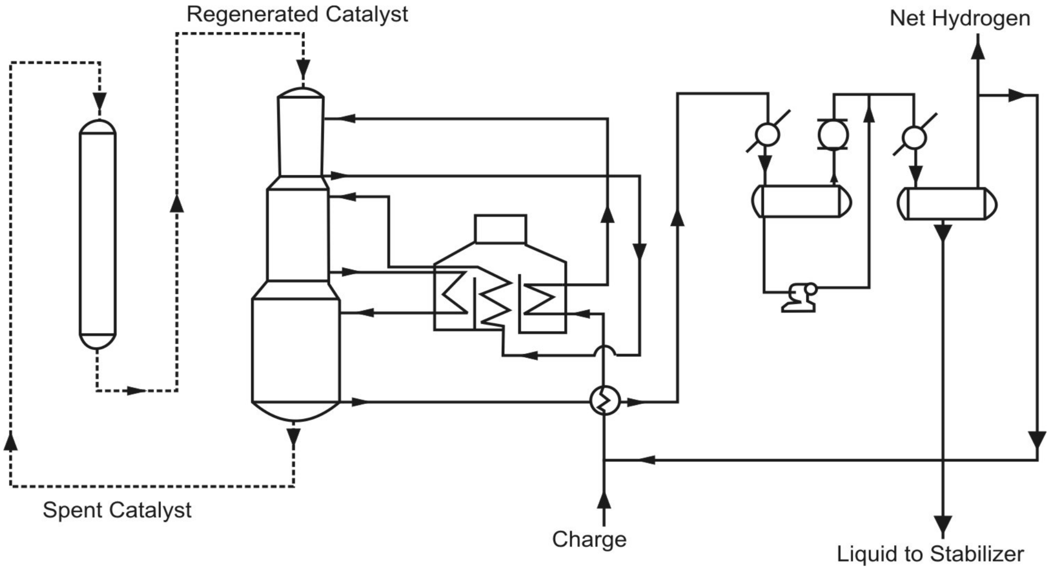

Figure 1: Catalytic Reforming Unit (PHRC, 1990)

The naphtha feed is first sent to the naphtha hydro-treating unit (NHU) where it is treated with hydrogen to remove sulphur, metals, olefins and nitrogen which could poison the catalyst (platinum) used in the reforming reactor. The desulphurised naphtha feed is preheated in a section of the furnace (charge heater) and fed with hydrogen from the recycle compressor to the first reactor, the effluent from the first reactor is then reheated in the first interheater and fed to the second reactor; finally, after reheating in the second interheater the effluent is fed to the third reactor. The effluent from the third reactor is used to preheat the unit feed, then cooled in air and water coolers and finally sent to a product separator where the effluent is separated into two phases; a liquid phase (reformate) and a hydrogen rich gaseous phase. The gas is partly recycled to the reactors, the net gas is split into two streams sent to the net gas wash section and to the booster compressors respectively. The reformate is debutanized and sent to storage. The final products are reformate, LPG, hydrogen, fuel gas and net gas. The catalyst (a bi-functional bimetallic catalyst such as Pt-Re/Al_2O_3) moves continuously from the first to the third reactor, from where it is withdrawn and sent to the regeneration section where it is regenerated continuously while the reactor circuit is on stream thus eliminated periodic shutdowns for in situ regenerations.

2. Materials and Methods

2.1. Model Development

To describe the operation of the catalytic reforming unit (CRU), a mathematical model of the reactor was developed from first principles by applying the principles of conservation of mass and energy. The following assumptions were made in the development of the model equations. The components in the reactor moves in a plug flow manner i.e. concentration varies along the length of the reactor bed, the reactor operates under steady state, reactions are in the same phase (homogenous reactions) and pressure drop effects along the reactor were neglected.

2.1.1. Kinetic Model

The naphtha feed to the reforming unit is a complex mixture of hydrocarbons consisting of several hundred components (Antons & Aitani, 2004) having below 15% aromatics and above 60% naphthenes – mixture of cyclopentanes and cyclohexanes (PHRC, 1990)) with each capable of undergoing various reactions (both desired such as dehydrogenation of naphthenes to aromatics, isomerisation of paraffins and naphthenes, dehydrocyclisation of paraffins to aromatics and undesired such as hydrocracking of paraffins to lower molecular weight compounds). The naphtha mixture is therefore usually idealized such that each of the three hydrocarbon classes; naphthenes, paraffins and aromatics was represented by a single compound with an average property of that class (Pseudo Components) and the reactions modelled as kinetic lumps. Various kinetic models of naphtha reforming have been proposed: the simplest is the four lumps model by Smith, (1959) where naphtha is composed of naphthenes, paraffins, aromatics and light hydrocarbons (<C5), with only four reactions. All other models can be described as extensions of the Smith's model and were aimed at accounting for more distinct components (lumps) in the complex naphtha feed. They include: Bommannan et al., (1989) model, similar to Smith's model but also considers catalyst deactivation.; Ramage, et al., (1980) the Mobil thirteen lumps model; Kmak, (1972) detailed (Exxon model) twenty-two lumps model; Ancheyta & Villafuerte, (2000) a twenty-four lumps model with 71 reactions, Froment, (1987) a twenty-eight lumps model with 81 reactions and Taskar & Riggs, (1997) thirty-five lumps model used for the optimization of semi-regenerative naphtha catalytic reformers. The kinetic models are a function of the number of components (lumps) and reaction paths of interest, with increasing number of lumps determining the complexity and a measure of the rigor of the model. The detailed models (with increasing numbers of lumps) are complicated as they require the estimation of more kinetic parameters (a function of the number of reaction paths). Hence a simple lumping scheme – the Smith's model with known reaction kinetics was chosen and used in this work.

2.1.2. Reaction Rate Expression

The reaction paths of the Smith's kinetic model for the three classes of compounds can be depicted as in Figure 2:

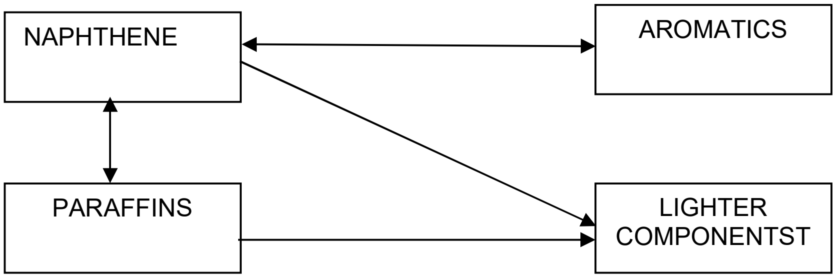

Figure 2: Reaction Path for the Smith's Kinetic Model

Reactions of catalytic naphtha reforming are elementary with reaction rates of each reaction path described by Hougen-Watson Langmuir - Hinshelwood type reaction rate expressions (Arani, et al., 2010) and the reaction rate coefficients obeying the Arrhenius law (Padmavathi, & Chaudhuri, 1997). The various reforming reactions, reaction path, reaction rate expression and rate constant expressions given by Askari, et al., (2012) and Mohaddecy & Sadighi. (2014) are as follows:

1. Dehydrogenation of naphthenes to aromatics: (highly endothermic)

$$Naphthenes \leftrightarrow \text{Aromatics} + 3\text{H}_2 \quad (1)$$

$$r_1 = \eta \rho_b k_{p_1}\left(P_N - P_A P_H^3 / K_{P_{1e}}\right) \quad (2)$$

$$k_{P_1} = exp(23.21 - 34750/1.8T) \quad (3)$$

$$K_{P_{1e}} = \frac{P_A P_H^3}{P_N} = exp(46.15 - 46045/1.8T) \quad (4)$$

2. Hydrocracking of naphthenes to paraffin: (endothermic reaction)

$$Naphthenes + H_2 \leftrightarrow \text{Paraffins} \quad (5)$$

$$r_2 = \eta \rho_b k_{p_2}\left(P_N P_H - P_H/K_{P_{2e}}\right) \quad (6)$$

$$K_{P_2} = exp(35.98 - 59600/1.8T) \quad (7)$$

$$K_{P_{2e}} = \frac{P_P}{P_N P_H} = exp(8000/1.8T - 7.12) \quad (8)$$

3. Hydrocracking of naphthenes to lower hydrocarbons (C1-C5)

$$C_nH_{2n}(naphthene) + \frac{n}{3}H_2 \rightarrow \frac{n}{15}\sum_{i=1}^{5} C_iH_{2i+2} \quad (9)$$

$$r_3 = \eta \rho_b K_{P_3}\frac{P_N}{P_t} \quad (10)$$

$$K_{P_3} = exp(42.98 - 62300/1.8T) \quad (11)$$

4. Hydrocracking of paraffins to lower hydrocarbons (C1-C5)

$$C_nH_{2n+2}(paraffins) + \frac{n-3}{3}H_2 \rightarrow \frac{n}{15}\sum_{i=1}^{5} C_iH_{2i+2} \quad (12)$$

$$r_4 = \eta \rho_b K_{P_4}\frac{P_P}{P_t} \quad (13)$$

$$K_{P_4} = exp(42.97 - 62300/1.8T) \quad (14)$$

Where: ρ_b is the bulk density of the catalyst (kg/m^3) and η is the catalyst effectiveness factor.

The values of η are: $0<\eta<1$; for new catalyst $\eta = 1$

The rate of reactions written for each specie following the reaction paths in Figure 2 are as follows:

Rate of reaction of Aromatics (r_A)

$$r_A = r_1 \rho_b \quad (15)$$

Rate of reaction of Naphthene (r_N)

$$r_N = \rho_b(r_1 - r_2 - r_3) \quad (16)$$

Rate of reactions of Paraffin (r_P)

$$r_P = \rho_b(r_2 - r_4) \quad (17)$$

Rate of reaction of H$_2$ (r_H)

$$r_H = \rho_b\left(3r_1 - r_2 - \frac{n}{3}r_3 + \frac{(n-3)}{3}r_4\right) \quad (18)$$

2.2 Reactor Model

Mass transfer occurring in each reactor was described using the principle of conservation of mass applied on a differential element of each catalyst bed. This yields the model equation for predicting the amount (mole) of any component in the naphtha feed along the length of the catalyst bed of each reactor as:

$$\frac{dN_i}{dL_{CB}} = A_R r_i \tag{19}$$

Where i = Aromatics, Naphthenes, Paraffins and Hydrogen.

N_i can be expressed in terms of mole fraction of component i as:

$$Y_i = \frac{N_i}{N_t} \tag{20}$$

The reactor cross sectional area A_R for a cylindrical reactor can be expressed as:

$$A_R = \pi r^2 \tag{21}$$

Substituting equations (20) and (21) into (19) gives the model equation in terms of the mole fraction of any component i as:

$$\frac{dY_i}{dL_{CB}} = \frac{\pi r^2}{N_t} r_i \tag{22}$$

Substituting the various rate equations into equation (22) gives the model equations for predicting the mole fractions of components in the naphtha feed as the reforming reaction occur along the catalyst bed of each reactor as:

$$\frac{dY_A}{dL_{CB}} = \frac{\rho_b \pi r^2}{N_t}\eta K_{P_1}\left(P_N - \frac{P_A P_H^3}{K_{P_1}}\right) \tag{23}$$

$$\frac{dY_N}{dL_{CB}} = \frac{\rho_b \pi r^2}{N_t}\left(-\eta K_{P_1}\left(P_N - \frac{P_A P_H^3}{K_{P_1}}\right) - \eta K_{P_2}\left(P_N P_H - \frac{P_H}{K_{P_2}}\right) - \eta K_{P_3}\frac{P_N}{P_t}\right) \tag{24}$$

$$\frac{dY_P}{dL_{CB}} = \frac{\rho_b \pi r^2}{N_t}\left(\eta K_{P_2}\left(P_N P_H - \frac{P_H}{K_{P_2}}\right) - \eta K_{P_4}\frac{P_P}{P_t}\right) \tag{25}$$

$$\frac{dY_H}{dL_{CB}} = \frac{\rho_b \pi r^2}{N_t}\left(3\eta K_{P_1}\left(P_N - \frac{P_A P_H^3}{K_{P_1}}\right) - \eta K_{P_2}\left(P_N P_H - \frac{P_H}{K_{P_2}}\right) - \frac{n}{3}\eta K_{P_3}\frac{P_N}{P_t} - \frac{(n-3)}{3}\eta K_{P_4}\frac{P_P}{P_t}\right) \tag{26}$$

The Temperature profile in each reactor was obtained by applying the principle of conservation of energy on a differential element of each catalyst bed. This gave the model equation for predicting the temperature progression along the length of the catalyst bed of each reactor as:

$$\frac{dT}{dL_{CB}} = \frac{\pi r^2}{\sum \dot{M}_i C_{p_i}} \sum_{j=1}^{n}\left(-\Delta H_{fj}\right) r_j \tag{27}$$

Where: ΔH_{fj} is the heat of reaction (Kj/Kmol H_2) for reaction path j
i = Aromatics, Naphthenes, Paraffins, Hydrogen; j = 1, …4

Substituting the heats of reaction for the various reaction paths into equation (27) gives:

$$\frac{dT}{dL_{CB}} = \frac{\pi r^2}{\sum \dot{M}_i C_{p_i}}\left(3r_1\left(-\Delta H_{f1}\right) + r_2\left(-\Delta H_{f2}\right) + \frac{n}{3}r_3\left(-\Delta H_{f3}\right) + \frac{(n-3)}{3}r_4\left(-\Delta H_{f4}\right)\right) \tag{28}$$

Substituting the rate equations for the various reaction paths into equation (28) gives:

$$\frac{dT}{dL_{CB}} = \frac{\pi r^2}{\sum \dot{M}_i C_{p_i}}\Bigg(3K_{p_1}\left(P_N - P_A P_H^3 / K_{P_1}\right)\left(-\Delta H_{f1}\right) + K_{p_2}\left(P_N P_H - P_H / K_{P_2}\right)\left(-\Delta H_{f2}\right) +$$

$$\frac{n}{3}K_{P_3}\frac{P_N}{P_t}\left(-\Delta H_{f3}\right)+\frac{(n-3)}{3}K_{P_4}\frac{P_P}{P_t}\left(-\Delta H_{f4}\right)\Bigg) \tag{29}$$

3. Methods

The component Partial Pressures in the model equations were converted to molar concentrations using the expression:

$$P_i = PY_i \tag{30}$$

Substitution of equation (30) of the various species into equations 23, 24, 25, 26 and 29) gives the model equations in terms of molar concentration. The developed model equations were a set of five coupled ordinary differential equations. The MatLab 7.5 ODE45 solver from Mathworks for non-stiff ordinary differential equations which uses the 4th order Runge Kutta algorithm was employed in solving the resulting ordinary differential equations. The accuracy of the developed models was ascertained using industrial plant data of the catalytic reforming unit of the Port-Harcourt Refining Company, Rivers State, Nigeria as input data in the solution of the model equations. The industrial reforming unit operates with three (3) cylindrical catalyst bed reactors of different diameters. The outputs (results) from the first reactor were used as inputs into the successive reactor and the process re-initiated. This was done for all three (3) catalyst bed reactors to obtain the concentrations of the components of the reforming reactions and outlet bed temperature along the catalyst bed of each reactor. To ensure reaction proceeds at optimum conditions, heaters are usually placed between the reactors to raise the inlet temperature of successive reactors to pre-determined optimum reaction temperature. Hence to replicate the industrial reactor accurately, the entry temperature values of the industrial reactors were used as inlet temperature values for the model equations The simulation of the reactors to study the effects of process variables was therefore performed on the first reactor only.

3.1. Determination of model parameters

To solve the model equations developed required the determination of certain constants and parameters in the model. These parameters and constants were determined as follows:

i. Determination of Heat Capacity

The specific heat capacities of the species were calculated using the formula in Liang *et al.*, (2005):

$$C_{pi} = 4.1868(a + bT + cT^2 + dT^3) \tag{33}$$

Where a, b, c and d are constants with values as listed in Table 1 (Liang *et al.*, 2005)

ii. Determination of Feed Properties and Operating Conditions

Feed composition and reactor bed properties from an industrial reforming process, the Port-Harcourt Refining Company at Alesa-Eleme Rivers State, Nigeria are given in Table 1.

Table 1: Operating Condition for Reforming Reactor (PHRC, 1990)

A. PROPERTIES OF NAPHTHA FEEDSTOCK

Density	766.6 kg/m^3
Feed rate	33,000 bpd (design)
Total Paraffin (vol.%)	36.4
Total Naphthenes (vol.%)	51.6
Total Aromatics (vol.%)	12.0
Density of Aromatics	873.8 kg/m^3
Density of Paraffin	6540.8 kg/m^3
Density of Napthene	779 kg/m^3
Catalyst Density	300 kg/m^3
Total Pressure	15 kg/cm^2

B. COEFFICIENT FOR FEED HEAT CAPACITY (Liang *et al.*, 2005)

Components	a	b x10^3	c x10^6	d x10^9
H_2	6.483	2.215	-3.298	1.826
P	-1.456	182.4	-100.24	21.15
N	-14.789	187.3	-106.0	22.37
A	-5.817	122.4	-66.05	11.73

C. REACTOR SPECIFICATION (PHRC, 1990)

Parameter	Reactor 1	Reactor 2	Reactor 3
Length (m)	4.1	4.1	4.1
Diameter	2.1	2.5	3.3
Inlet Pressure (kg/cm^2)	9.84	9.28	8.73
Inlet Temperature (K)	798	798	798
Outlet Temperature (K)	713	753	773
Temperature Drop (K)	85	45	25

D. HEAT OF REACTION: Liang *et al.*, (2005):

Reaction Path	ΔH_{f1}	ΔH_{f2}	ΔH_{f3}	ΔH_{f4}
Heat of Reaction (kJ/kmol. H_2)	71038.06	-36953.33	-56597.54	-51939.31

4. Discussion of Results

The results obtained from the solution of the model equations are presented below,

4.1. Mole Fractions of each Lump Specie (Naphthenes, Aromatics, Paraffine) and Hydrogen

The concentration profile of each lumped class (Naphthenes, aromatics and paraffins) and hydrogen across the three reactor beds and the net amounts of these components used or produced during the reforming reaction in the reactor beds are shown in Figure 3 and Table 2 respectively.

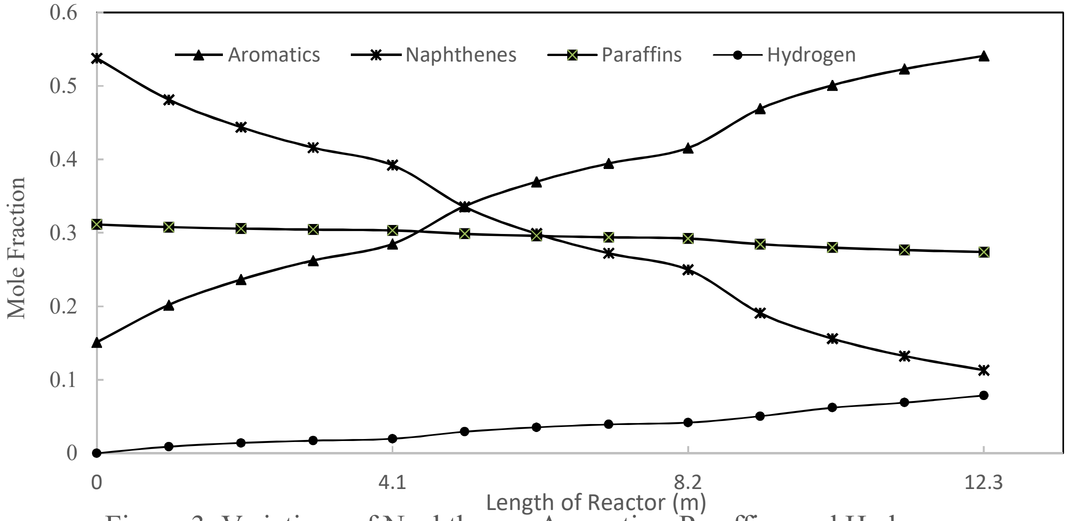

Figure 3: Variations of Naphthenes, Aromatics, Paraffins and Hydrogen mole fractions along the reactor Beds

Table 2: Amount of Reactants used and Products produced in each Reactor

COMPONENT	PARAMETER	REACTOR 1	REACTOR 2	REACTOR 3	FEED CONC.
NAPHTHENE	OUTLET CONC.	0.3920	0.2497	0.1131	0.5376
	AMOUNT USED	0.1456	0.1423	0.1366	
AROMATICS	OUTLET CONC.	0.2849	0.4156	0.5410	0.1511
	AMOUNT PRODUCED	0.1338	0.1307	0.1256	
PARAFFIN	OUTLET CONC.	0.3033	0.2923	0.2739	0.3113
	AMOUNT USED	0.008	0.011	0.0184	
HYDROGEN	AMOUNT PRODUCED	0.0197	0.0417	0.0787	0

The main reforming reactions are dehydrogenation and hydrocracking of naphthenes to aromatics (Taskar, 1996); the model as shown in Figure 3 predicts a decrease in the concentrations of naphthenes and paraffins (Kohnehshahri, et al., 2011) due to isomerization and hydrocracking reactions. Thus increasing the aromatics concentration as reaction proceed along the reactor beds. Table 2 shows the net amounts of naphthenes, paraffins, aromatics and hydrogen used or produced as the reforming reaction occurs from reactors 1 to 3. The amount of naphthenes used and the amount of aromatics formed both decreased from reactors 1 to 3, an indication that dehydrogenation and hydrocracking reactions of naphthenes were highest in reactor 1 and decreased as reaction proceeds in reactor 2 and 3. The amount of paraffins used increased as the reforming reaction occurs from reactors 1 to 3 as the hydrocracking of paraffins are considered the slowest of the reforming reaction with reaction rates increasing as reaction proceed from reactor 1 to 3 (Arani, et al., 2009). Figure 3 also showed that the concentration of Hydrogen increased across all the three reactor beds. This is in agreement with the work of Zaidoon, (2011) who reported increased hydrogen molar flow rates in the four reactors of his model in spite of difference in reaction types, the hydrogen yield for a given naphtha feedstock being determined by the balance between hydrogen producing and hydrogen consuming reactions (Ali, et al., 2006).

4.2. Temperature Profiles

The predicted temperature profiles along the lengths of the three reactor beds are shown in Figure 4. The exit temperatures of each reactor and the corresponding temperature gradient when compared to the entry temperatures are shown in Table 3.

Table 3: Entry, Outlet Temperature and Gradient of each Reactor

	REACTOR 1	REACTOR 2	REACTOR 3
ENTRY	798	798	798
OUTLET (MODEL)	715.38	760.21	772.98
GRADIENT	82.62	37.79	25.02

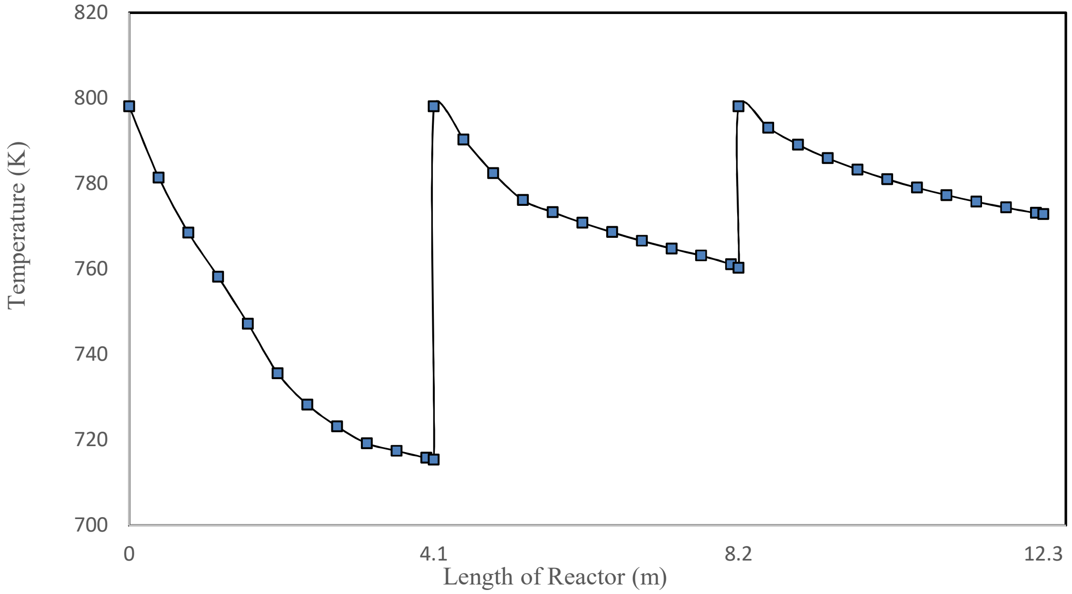

Figure 4: Temperature Profiles along the Reactor

The main reforming reactions (dehydrogenation and hydrocracking of naphthenes) are highly endothermic (Taskar, 1996), absorbing heat in the course of reaction resulting in a decrease in temperature as reaction proceeds. Hu, et al., (2003) and Weifeng, et al., (2006) also observed that as the feedstock passes through the sequence of heating and reacting, the reactions become less endothermic and temperature difference across the reactors decrease. These trends were accurately predicted by the model as shown in Figure 4; a decrease in temperature along all reactor beds with the largest decrease in reactor 1 and a successive reduction of the gradient in reactors 2 and 3 (82.62K, 37.79K and 25.02K) as shown in Table 3. In reactor 1, the main reactions (Ancheyta, et al., 2001): cycloalkane aromatization - dehydrogenation of paraffins and naphthenes to aromatics are endothermic reactions (Arani, et al., 2009) and results in a large bed temperature drop of this reactor. Similar result was obtained by Kohnehshahri, et al., (2011). In reactors 2 and 3, dehydrogenization reaction (endothermic); dehydrocyclization, and hydrocracking reactions (exothermic) (Zaidoon, 2011) and aromatization of cycloalkane produced through cyclization reaction (endothermic) (Liang, et al., 2005) all occur. The dynamics of these exothermic and endothermic reactions results in successive drop of the bed temperature in these two reactors with reduced temperature gradient and increased outlet temperature as reaction progresses.

4.3. Model Validation

The comparison of the model results with those of the industrial data from the reforming unit of the Port-Harcourt refinery are presented in Table 4.

Table 4: Comparison of Model Results and Industrial Data

Parameter	Plant Value	Model Prediction	Percentage Absolute Error (Deviation) %
Aromatics Concentration	0.53	0.5410	2.1
Naphthenes Concentration	0.12	0.1131	5.8
Paraffins Concentration	0.35	0.2739	2.2
Hydrogen Concentration	0.08	0.0787	1.6
Temperature (K)	773	772.98	0.0026

Table 4 shows that the maximum percentage absolute error (deviation) between the model predictions and output from the plant is 5.80%. Therefore, the model developed can be used for simulation studies of the catalytic bed reactors of the reforming unit.

4.4. Process Simulation

The catalyst bed of Reactor 1 was selected for simulation studies. The effects of the following process variables on the performance of the reforming reactors were studied.

A. Effect of Inlet Temperature

The effects of variation in inlet temperature on the output concentration (mole fraction) and outlet temperature of reactor 1 are shown in Figures 5 and 6.

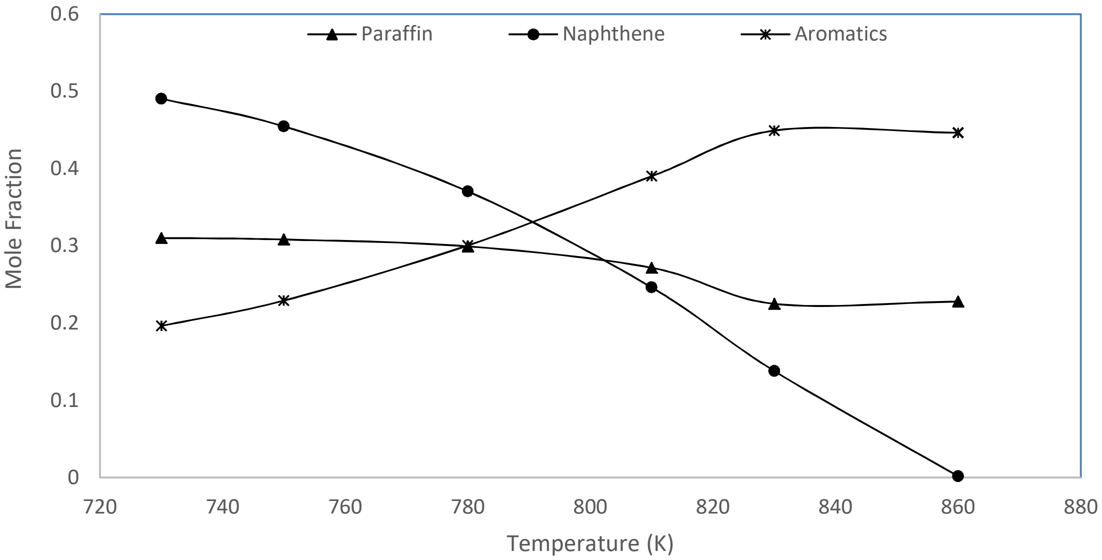

Figure 5: Effect of Inlet Temperature on Mole Fractions at the Reactor 1 outlet

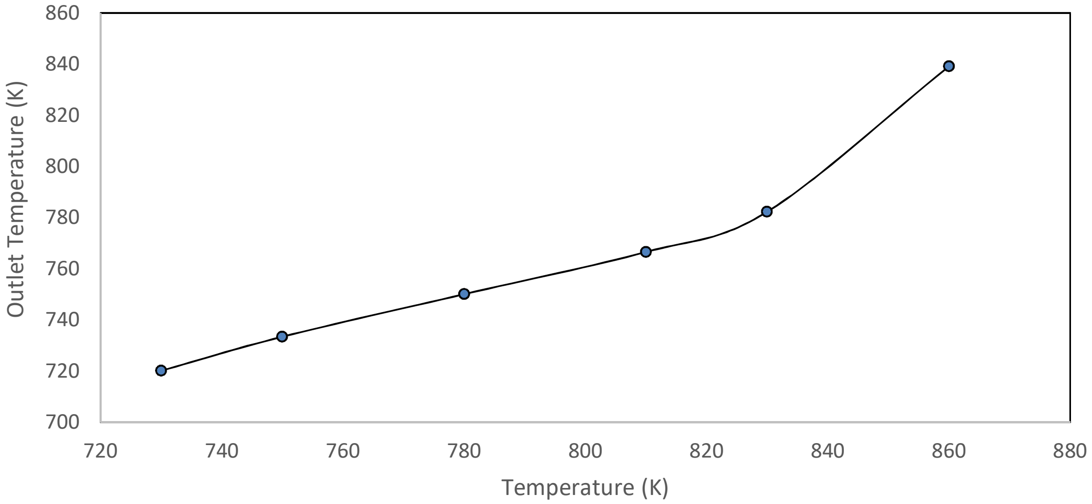

Figure 6: Effect of Inlet Temperature on outlet Temperature of Reactor 1

Increase in inlet temperature increases the rate of reforming reaction, however; Rahimpour, (2006) reported that very high inlet temperatures result in high coke formation, reducing catalyst activity leading to reduced reforming reaction. This Figure 5 shows accurately; an increase in aromatics concentration, reaching a maximum at an inlet temperature of 830K, beyond this temperature, (very high temperature) aromatics concentration began to decrease; the concentration of naphthene decreases continuously but more sharply at 830K, while the concentration of paraffin decreases, reaches a minimum at 830K and increased thereafter. Figure 6 shows that as the inlet temperature in reactor 1 is increased, the outlet temperature increases; with higher increase beyond inlet temperature of 830K. This is due to the sharp drop in endothermic reforming reactions resulting from decreased catalyst activity due to coke formation at high inlet temperatures and an increasing degree of hydrocracking reactions which are exothermic in nature (Taskar, 1996).

B. Effect of Reactor Pressure

The effects of Pressure on the output concentration (mole fraction) and outlet temperature of reactor 1 are shown in Figures 7 and 8.

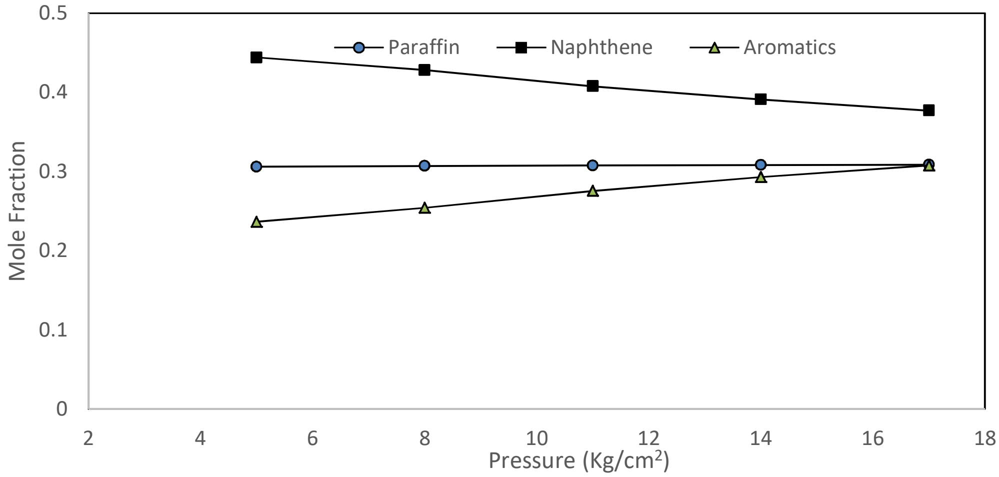

Figure 7: Effect of Pressure on Mole Fraction at the Reactor outlet

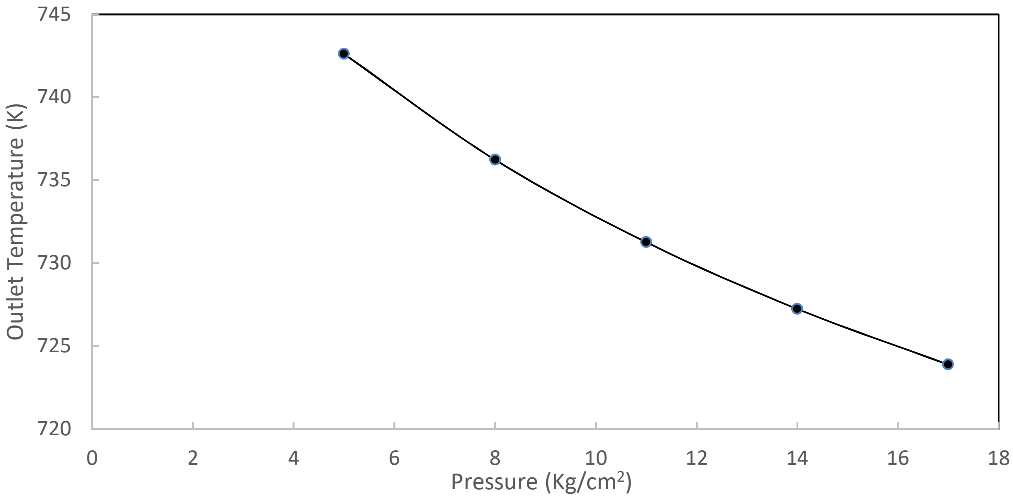

Figure 8: Effect of Pressure on Reactor 1 outlet temperature

Increased pressure increases the rate of reaction. Thus more reactants are used and more products formed as shown in Figure 7 where the concentration of aromatics increased while those of naphthene and paraffin reduced. Similar results of decrease in naphthenes mole fraction and increase in aromatics mole fraction with increase in pressure were reported by Elsayed, et al., (2016) and minimal increase in aromatics yield by Mohhaddecy & Sadighi, (2015). This trend was explained by Turaga and Ramanathan, (2003) to be due to faster dehydrogenation of naphthenes and dehydrocyclization of paraffin's to aromatics at increased pressures. The effect of pressure on the outlet temperature (Figure 8) show that outlet reactor temperature decreases as pressure increase. This is due to the increased endothermic reaction with increased pressure which absorbs heat resulting in a reduction in final temperature.

C. Effect of Feed Flowrate

The effects of feed flow rate on the output concentration (mole fraction) and outlet temperature of reactor 1 are shown in Figures 9 and 10.

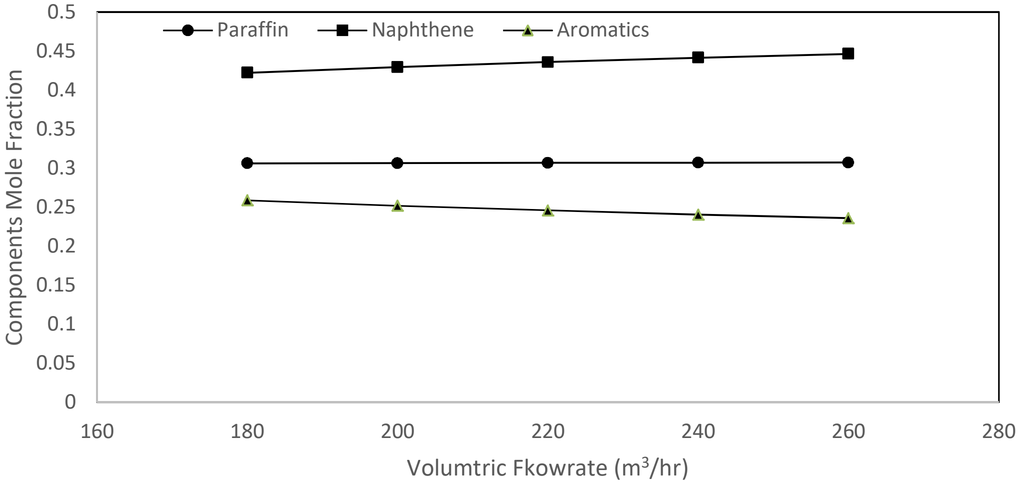

Figure 9: Effect of Feed Flow Rate on Mole Fractions at the Reactor outlet

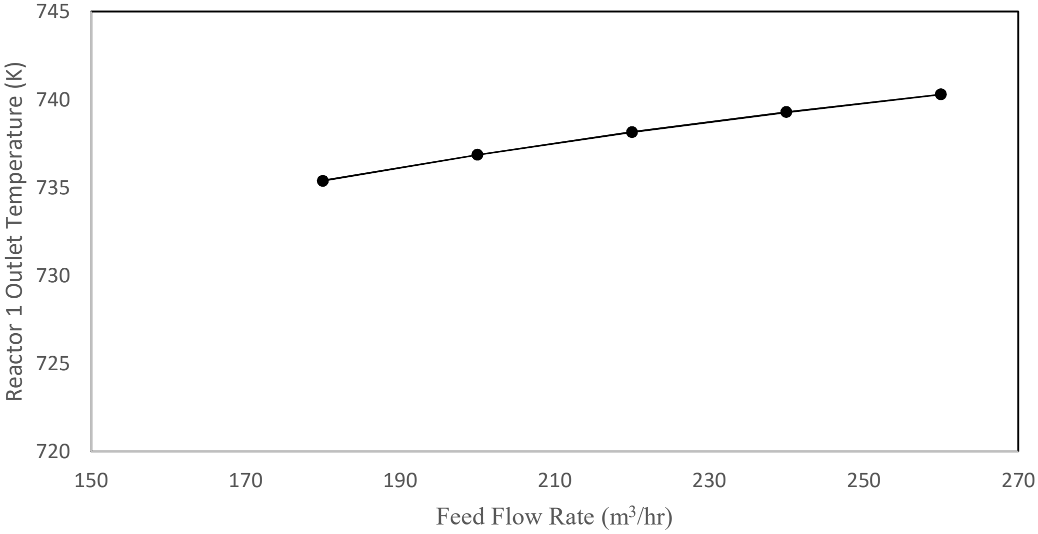

Figure 10: Effect of Feed Flow Rate on Reactor 1 Outlet Temperature

Increasing the feed flow rate increases the velocity of flow of the feed components (naphthene and paraffin) in the reactor, thus the feed components spend less time in the reactor (reduction in contact time) and more reactants leave the reactor un-reacted. Hence the concentration of the reactants increases, that of the product (aromatics) reduces with increased feed flow rate as shown in Figure 9. Since increased feed flow rate reduces rate of reaction, the reduced rate of reaction means less heat will be absorbed as feed flow rate increases resulting in an increase in the outlet temperature of the reactor as shown in Figure 10.

5. Conclusion

Models for the simulation of the reactors of a catalytic reforming unit were developed. The models could predict the concentration of reactants, product and temperature progression along the reactor beds of the catalytic reforming reactors. To evaluate the developed model, the results were compared against industrial plant data of the catalytic reforming reactor of the Port-Harcourt Refinery, Rivers State, Nigeria. The percentage absolute error (deviation) of the concentrations of Aromatics, Naphthene, Paraffin, Hydrogen and outlet temperature were 2.1%, 5.8%, 2.2%, 1.6% and 0.0026% respectively. These results show a close mapping between the model predictions and the industrial data, hence the models can be reliably used for simulation studies of the catalytic reforming unit. Three process variables were studied and their effects on the reformate composition are as follows: Increasing the inlet feed temperature increases aromatic yield reaching a maximum at 830K (557°C); Increasing the total pressure increases aromatic yield (though minimal) in the reformate; Increasing the feed flow rate decreases aromatic yield (though minimal) in the reformate.

References

Ali S. A., Siddiqui M. A., Mohammed, A. A., (2006), "Parametric Study of Catalytic Reforming Process", J. React. Kinet. Catal. Litt, 87 (1), 199 – 206.

Arani, H. M., Shokri, S. & Shirvani, M. (2010), Dynamic Modeling and Simulation of Catalytic Naphtha Reforming, International Journal of Chemical Engineering and Applications, 1, (2), 159 – 164.

Arani, H., Shirvani, M. M., Safdarian, K. & Dorostkar, E. (2009). Lumping Procedure for a Kinetic Model of Catalytic Naphtha Reforming, Brazilian Journal of Chemical Engineering, 26, (04), 723 – 732.

Ancheyta, J., Villafuerte, E., Diaz, L. & Gonzalez, E., (2001), 'Modeling and Simulation of Four Catalytic Reactors in Series for Naphtha Reforming, Energy Fuels, 15, 887-893.

Ancheyta-Juarez, J. & Villafuerte-Macias, E., (2000), Kinetic Modeling of Naphtha Catalytic Reforming Reactions, Energy & Fuels, 14, (5), 1032 – 1037.

Antons, G. A. & Aitani, A. M. (2004), Catalytic Naphtha Reforming, Mercel Dekker Inc.

Askari, A., Karimi, H., Ruhimi, R. M. & Ghanbari, M., (2012), “Simulation and Modelling of Catalytic Reforming Process”. Petroleum and Coal 54(1), 76 - 84.

Bommannan, D. Srivastava, R. D. & Saraf, D. N. (1989), Modelling of catalytic naphtha reformers, Can. J. Chem. Eng., 67. 405 - 411.

Elsayed, H. A., Menoufy, M. F., Shaban, S. A., Ahmed, H. S. & Heakal, B. H. (2016), Optimization of the reaction parameters of heavy naphtha Reforming Process using Pt-Re/Al2O3 catalyst system, Egyptian Journal of Petroleum, https://doi.org/10.1016/j.ejpe.2015.03.009

Froment, G. F. (1987), Modelling of Catalytic Reforming Unit"; Chem.Eng.Sci., 42, 1073 - 1087.

Gary, J. H., Handwerk, G. E. & Kaiser, M. J. (2006), Petroleum Reforming Technology and Economics, 5th Edition, CRC Press, Taylor and Francis group, New York.

Hu Y. Y., Su. H. Y. & Chu. J., (2003), Modeling and Simulation of Commercial Catalytic Reformers, J. of Chem. Eng. of Chines Univ, 17, 418 - 424.

Kohnehshahri, R. K., Mohaddeay, S. R. S., Salami, M. & Shirazran, S. (2011), Modeling and numerical Simulation of catalytic Reforming Reactor, Oriental J’ournal of Chemistry, 27, (4), 1351 - 1355.

Kmak, W. S. (1972), A Kinetic Simulation Model of the Power Forming Process, AIChE Meeting, Houston, TX.

Liang, K. Guo, H. & Pan, S. (2005), A study on naphtha catalytic Reforming Reactor simulation and analysis, Journal of Zhejoang Uni Sc., 6B, (6), 590 - 596.

Mohaddecy, S. R. & Sadighi, S. (2014), Developing a Steady-state Kinetic Model for Industrial Scale Semi-Regenerative Catalytic Naphtha Reforming Process, Kem. Ind. 63 (5-6) 149 – 154.

Mohaddecy, S. R. & Sadighi, S. (2015), Modelling Catalytic Naphtha Reforming process using discrete lumping approach, Indian Journal of Chemical Technology, 21, 309 – 320.

Mohaddecy S. R., Zahedi S, Sadighi, S. & Bonyad, H. (2006), Reactor Modelling and Simulation of Catalytic Reforming process, Petroleum and Coal, 48, (3), 28 - 35.

Padmavathi, G. & Chaudhuri, K. K. (1997), Modeling and Simulation of Commercial Catalytic Naphtha Reformer, Can. J. Chemical Engineering, 75, (10), 930 - 937.

PHRC, (1990), Port-Harcourt Refinery Company Specific Gourse for Junior Staff Process, General Index, Vol.1/B, 1302 NPHR Area 2 Process Description 1302-45 – 103.

Rahimpour, M. R. (2006), Operability of an Industrial Catalytic Naphtha Reformer in the presence of catalyst deactivation, Chem. Eng. Technol., 29, 616 - 624.

Ramage, M. P., Graziani, K. R. & Krambeck, F. J., (1980), Development of Mobil's Kinetic Reforming Model, Chemical Engineering Sci., 35, 3541 - 48.

Smith, R. B. (1959), Kinetic analysis of naphtha reforming with platinum catalyst, Chem. Eng. Prog., 55, 76 - 80.

Taskar, U. M., (1996), Modeling and Optimization of a catalytic Naphtha reformer, Ph.D. Dissertation Texas Tech. University.

Taskar, U. & Riggs, J. B., (1997), Modeling and Optimization of a Semi-Regenerative Catalytic Naphtha Reformer, AIChE J., 43, (3), 740 - 753

Turaga, U. T. & Ramanathan, R., (2003), Catalytic Naphtha Reforming: Revisiting Its Importance in the Modern Refinery, Journal of Scientific & Industrial Research 62, 963 – 978.

Weifeng, H., Hongye, S., Hongyou, H. & Jain, C., (2006), 'Modeling, Simulation and Optimization of a Whole Industrial Catalytic Naphtha Reforming Process on Aspen Plus Platform, Chin. J. Chem. Eng, 14, (55), 584 - 591.

Zaidoon M. S., (2011), Catalytic Reforming of Heavy Naphtha, Analysis and Simulation, Diyala Journal of Engineering Sciences, 04, (02), 86 – 104.

NUMENCLATURE

A = Aromatics
A_R = Reactor cross sectional area
C_{P_i} = Heat capacity of component i J $Mol^{-1}K^{-1}$
H = Hydrogen
i = Component A, N, P, H
j = Reaction path 1, 2, 3, 4
K_{P_i} = Reaction rate constant
$K_{P_{i_e}}$ = Equilibrium constant
L_{CB} = Length of catalyst bed m
$\dot{M}_\iota$ = Mass flowrate of Component I Kg sec^{-1}
N = Napthene
n = Number of atoms
P = Paraffin
P_i = Partial Pressure of Hydrogen atm

P_T = Total Pressure of Column atm
ρ_b = Bulk Density of Catalyst Kgm^{-1}
r_i = Rate of Reaction of component i
r = Reactor radius m
T = Temperature K
Y_i = Mole Fraction of Component i
ΔH_{f_j} = Heat of Reaction for reaction path j KJ Kmol^{-1}
η = Catalyst effectiveness factor